

Design of Robust Control Systems for a Hypersonic Aircraft

Christopher I. Marrison* and Robert F. Stengel†
Princeton University, Princeton, New Jersey 08544

Robust flight control systems are synthesized for the longitudinal motion of a hypersonic aircraft. Aircraft motion is modeled by nonlinear longitudinal dynamic equations containing 28 uncertain parameters. Each controller is designed using a genetic algorithm to search a design coefficient space; Monte Carlo evaluation at each search point estimates stability and performance robustness. Robustness of a compensator is indicated by the probability that stability and performance of the closed-loop system will fall within allowable bounds, given likely parameter variations. A stochastic cost function containing engineering design criteria (in this case, a stability metric plus 38 step-response metrics) is minimized, producing feasible control system coefficient sets for specified control system structures. This approach trades the likelihood of satisfying design goals against each other, and it identifies the plant parameter uncertainties that are most likely to compromise robustness goals. The approach makes efficient use of computational tools and broadly accepted engineering knowledge to produce practical control system designs.

Nomenclature

a	= speed of sound, ft/s
C_D	= drag coefficient
C_L	= lift coefficient
$C_M(q)$	= moment coefficient due to pitch rate
$C_M(\alpha)$	= moment coefficient due to angle of attack
$C_M(\delta E)$	= moment coefficient due to elevator deflection
C_T	= thrust coefficient
\bar{c}	= reference length, 80 ft
D	= drag, lbf
h	= altitude, ft
I_{yy}	= moment of inertia, 7×10^6 slug-ft ²
L	= lift, lbf
M	= Mach number
M_{yy}	= moment about pitch axis, lbf-ft
m	= mass, 9375 slugs
q	= pitch rate, rad/s
R_E	= radius of the Earth, 20,903,500 ft
r	= radial distance from Earth's center, ft
S	= reference area, 3603 ft ²
T	= thrust, lbf
V	= velocity, ft/s
α	= angle of attack, rad
β	= throttle setting
γ	= flight-path angle, rad
δE	= elevator deflection, rad
μ	= gravitational constant, 1.39×10^{16} ft ³ /s ²
ρ	= density of air, slugs/ft ³

Introduction

HYPERSONIC flight presents a difficult challenge for control design. High velocity causes the aircraft to be very sensitive to changes in the flight condition. For example, at an altitude of 110,000 ft and a Mach number of 15 (velocity of 15,060 ft/s), a 1-deg increase in angle of attack produces a normal acceleration of 11.5 ft/s², i.e., a load factor of about $\frac{1}{3}$ g. For typical configurations, the phugoid mode is lightly damped or unstable, the short-period mode is unstable, and thrust magnitude is very sensitive to small changes in angle of attack. The problem is compounded by the difficulty of measuring atmospheric properties and of estimating aerodynamic characteristics. Nevertheless, a hypersonic aircraft's

flight control system must ensure that the aircraft is always stable, that response to commands from a pilot or autopilot is satisfactory, and that external disturbances do not produce unacceptable aircraft motions. This paper addresses the design of such control systems, with particular attention devoted to achieving robustness in the face of parameter uncertainty.

Stochastic robustness analysis quantifies the lack of robustness of a compensator \mathcal{G} by the probability P that variations in plant parameters will cause the closed-loop system to have unacceptable behavior. This simple concept of probability is defined mathematically as the integral of an indicator function over the space of expected parameter variations:

$$P = \int_{\mathcal{V}} I[\mathcal{H}(\nu), \mathcal{G}] \text{pr}(\nu) d\nu \quad (1)$$

\mathcal{H} describes the plant, i.e., the dynamic model of the aircraft; \mathcal{V} is the space of possible plant parameter variations; ν is a specific point in \mathcal{V} ; and $\text{pr}(\nu)$ is the probability density function of ν . $I(\cdot)$ is a binary indicator function that equals zero if $\mathcal{H}(\nu)$ and \mathcal{G} form an acceptable system and equals one if the system is unacceptable. The division of the space into acceptable and unacceptable regions is illustrated in Fig. 1. The definition of unacceptable is at the designer's discretion; for example, it can mean instability, violation of a response envelope, or excess control usage. A probabilistic design metric is equally applicable to systems that are linear or nonlinear, time-varying or time-invariant, continuous or discrete.

In most applications, Eq. (1) cannot be integrated analytically. Monte Carlo evaluation (MCE)¹ is a practical alternative, with $\text{pr}(\nu)$ used to shape the random samplings of values for the uncertain parameters ν . Individual selections for each trial are denoted ν_k . At each ν_k , the closed-loop characteristics of the system are tested for acceptability. For example, a linear system's stability indicator function is set equal to one if any of the closed-loop eigenvalues have positive real parts and is set equal to zero otherwise. A performance indicator function, e.g., step-response overshoot or settling time, is set to one if a design limit is exceeded or to zero if it is not. The trials are repeated for N samples from the space \mathcal{V} , the value of N being chosen to obtain the required accuracy. A probability estimate is expressed as

$$\hat{P} = \frac{1}{N} \sum_{k=1}^N I[\mathcal{H}(\nu_k), \mathcal{G}] \quad (2)$$

and the estimate approaches the exact value in the limit as $N \rightarrow \infty$. Performance and stability probability estimates can be combined not only to portray control system robustness but to design robust controllers.²⁻¹⁰

Defining the best compensator for a particular application is a subjective process, involving tradeoffs between possibly disparate

Received Jan. 9, 1996; revision received May 29, 1997; accepted for publication July 1, 1997. Copyright © 1997 by the American Institute of Aeronautics and Astronautics, Inc. All rights reserved.

*Graduate Student, Department of Mechanical and Aerospace Engineering; currently Consultant, Oliver, Wyman & Co., New York, NY 10103.

†Professor, Department of Mechanical and Aerospace Engineering. Fellow AIAA.

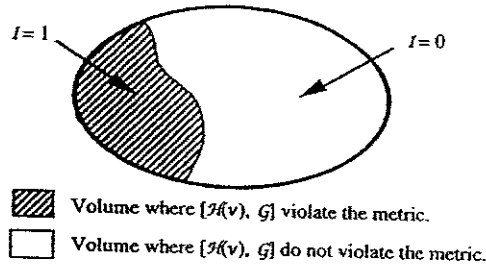


Fig. 1 Division of the space of uncertain parameters.

measures of stability and performance. These tradeoffs can be formalized by combining the individual probabilities in a scalar cost function J with each probabilistic measure assigned a subjective weighting. If the compensator \mathcal{G} is parameterized by a vector of design constants d , then P and J are functions of d , and robust control systems are designed by minimizing the cost function

$$\hat{J}(d) = \sum_{m=1}^M [w_m \hat{P}_m^2(d)] \quad (3)$$

where M is the number of stability and performance metrics, $\hat{P}_m(d)$ is the m th metric, and w_m is the weight on the m th metric. Robust compensators were designed for a linear benchmark control problem using a line search in Ref. 10 and a genetic algorithm (GA) in Ref. 11 to estimate the minimum of $J(d)$. The resulting compensators were highly robust, the probabilities of failure being significantly less than those of controllers created by other methods.⁸ The line search in Ref. 10 was effective but inefficient; the GA reduced search computation by an order of magnitude.¹¹

Stochastic robustness analysis and design provide a direct extension of classical design methods because stability and performance indicator functions are based on classical metrics. If frequency-domain measures were of interest, they could be added easily to the design cost. Nevertheless, we caution that gain and phase margins are unreliable indicators of robustness.⁹ The reason is quite simple: Realistic parameter variations, such as those considered here, produce not only gain and phase margin variations but changes in the shape of the Nyquist plot as well. Maximum singular values are essentially multivariate gain margins and have limited robustness interpretations for the same reason.⁷

In this paper, MCE and a GA¹²⁻¹⁵ are applied to a complex problem: flight control of a hypersonic aircraft cruising at a Mach number of 15 at an altitude of 110,000 ft. The dynamic model describes motions in the vertical plane, and it contains important nonlinear effects. We consider 39 stability and performance robustness metrics, significantly more than can be accommodated in other robust design techniques. The design approach is demonstrated at a single cruising flight condition, and it could be applied easily at other flight conditions, extending results over the full flight envelope via gain scheduling.

Hypersonic Aircraft Model

The longitudinal equations of motion include both an inverse-square-law gravitational model and the centripetal acceleration that results from a curved flight path. At Mach 15 and 110,000 ft, the non-rotating-Earth centripetal acceleration is 10.8 ft/s². The fifth-order equations for velocity, flight-path angle, altitude, angle of attack, and pitch rate are, respectively,

$$\dot{V} = \frac{T \cos \alpha - D}{m} - \frac{\mu \sin \gamma}{r^2} \quad (4)$$

$$\dot{\gamma} = \frac{L + T \sin \alpha}{mV} - \frac{(\mu - V^2 r)}{V r^2} \quad (5)$$

$$\dot{h} = V \sin \gamma \quad (6)$$

$$\dot{\alpha} = q - \dot{\gamma} \quad (7)$$

$$\dot{q} = M_{yy}/I_{yy} \quad (8)$$

The values of lift, drag, thrust, pitching moment, and radius from the Earth's center are modeled, respectively, by

$$L = \frac{1}{2} \rho V^2 S C_L \quad (9)$$

$$D = \frac{1}{2} \rho V^2 S C_D \quad (10)$$

$$T = \frac{1}{2} \rho V^2 S C_T \quad (11)$$

$$M_{yy} = \frac{1}{2} \rho V^2 S \bar{c} [C_M(\alpha) + C_M(\delta E) + C_M(q)] \quad (12)$$

$$r = h + R_E \quad (13)$$

The aerodynamic coefficients and air data are functions of the state and control, and interpolation of lookup tables or spline fits would be used in precise simulation. In this example, relatively simple functions were fitted to the data around the nominal cruising condition. Air-density and speed-of-sound models are taken from Ref. 16, and numerical values for the aerodynamic coefficients are representative of the NASA Langley Hypersonic Vehicle Simulation Model.¹⁷

For this design exercise, 28 inertial, thrust, and aerodynamic parameters are assumed to be uncertain, with v denoting an element of the uncertainty vector ν . The parameters are

$$m = v_1 m_0 \quad (14)$$

$$I_{yy} = v_2 I_0 \quad (15)$$

$$S = v_3 S_0 \quad (16)$$

$$\bar{c} = v_4 \bar{c}_0 \quad (17)$$

$$\rho = 0.00238 \exp\left(\frac{-h}{v_8 24,000}\right) \quad (18)$$

$$a = v_5 (v_6 8.99 \times 10^{-9} h^2 - v_7 9.16 \times 10^{-4} h + 996) \quad (19)$$

$$M = V/a \quad (20)$$

$$C_L = v_9 \alpha \left(0.493 + \frac{v_{10} 1.91}{M}\right) \quad (21)$$

$$C_D = v_{11} 0.0082 (v_{12} 171 \alpha^2 + v_{13} 1.15 \alpha + 2) \times (v_{14} 0.0012 M^2 - v_{15} 0.054 M + 1) \quad (22)$$

$$k = v_{16} 38 [1 - v_{17} 164 (\alpha - \alpha_0)^2] \left(1 + \frac{v_{18} 17}{M}\right)$$

$$C_T = k(1 + v_{19} 0.15) \beta \quad \text{if } \beta < 1 \\ = k(1 + v_{19} 0.15 \beta) \quad \text{if } \beta > 1 \quad (23)$$

$$C_M(\alpha) = 10^{-4} v_{20} [0.06 - e^{-v_{21} M/\beta}] [-2v_{22} \alpha^2 + 120v_{23} \alpha - 1] \quad (24)$$

$$C_M(q) = (\bar{c}/2V) q v_{24} (-0.025v_{25} M + 1.37) \times (-0.0021v_{26} \alpha^2 + 0.0053v_{27} \alpha - 0.23) \quad (25)$$

$$C_M(\delta E) = 0.00051 v_{28} (\delta E - \alpha) \quad (26)$$

Equations (4-26) define the plant model $\mathcal{H}(\nu)$. In this example, each v is assumed to follow a normal probability density function, with a mean of 1 and a standard deviation of 0.1; this defines $\text{pr}(\nu)$. For illustration, normally well-known quantities such as wing area and mean aerodynamic chord are treated as unknown. In application, realistic uncertainty values should be used; if uncertainties are sufficiently small, they could be ignored. Assuming normally distributed parameter uncertainty assures that the probability of instability will never be zero, as the tails of the parameter distributions

extend to plus or minus infinity. Setting each element of ν equal to one gives the nominal system. In MCE, each element of ν is produced by a separate call to a random-number generator on each trial. The method is not restricted to normal distributions; uncertainty can be represented by any appropriate distribution, including bounded (e.g., uniform), multimodal, or discrete distributions.

The linearized open-loop longitudinal dynamic model has eigenvalues of -0.895 , 0.784 , $-0.00021 \pm 0.0362j$, and 0.00011 at the trimmed cruise condition ($M = 15$, $h = 110,000$ ft, $\gamma = 0$ deg, and $q = 0$ deg/s). The trim (or equilibrium) condition is calculated using the nonlinear model, as noted. The first two eigenvalues represent a statically unstable short-period mode; the complex pair of eigenvalues portrays a lightly damped phugoid mode, and the last real eigenvalue indicates a mildly unstable height mode.¹⁸ Consequently, cruising flight would be subject to attitude and height divergences that would require stabilizing feedback control.

Nonlinear response histories are initiated at the equilibrium cruise condition, which is determined by finding the angle of attack, thrust, and elevator settings that provide force and moment balance in the nonlinear equations of motion for steady, level flight. Having established equilibrium, the command step is applied, and the state response is propagated using the nonlinear dynamic model. The state history then is evaluated with robustness performance metrics.

Stability and Performance Metrics

Three broad aspects of flight control robustness are of concern in this design study: stability, velocity command response, and height command response. They are expressed in a combination of 39 indicator functions. Stability in the neighborhood of the trim condition (metric 1) is predicated on the stability of the locally linearized system at that point, as determined by the eigenvalues of the closed-loop system.¹⁹ Nineteen additional metrics (2–20) are based on the response of the nonlinear model to a commanded step change in velocity of 100 ft/s. These are defined in Table 1. Double metrics such as $I_{V,T25}$ and $I_{V,T50}$ are used to allow the search to differentiate between compensators in the case in which both compensators constantly violate the more-demanding metric but only occasionally violate the less-demanding metric. The remaining 19 metrics (21–39) are based on the response to a commanded step change in height of 2000 ft. The height metrics are the same as the velocity metrics except that the times are doubled (and in the description, the subscript V is replaced by h). The cost function chosen to guide the design is the weighted quadratic sum

$$\hat{J}(d) = \sum_{m=1}^{39} [w_m \hat{P}_m^2(d)] \quad (27)$$

where the stability metric weight is 10, the basic performance metric weights are 1, and the more-demanding performance metric weights are 0.1.

As with all global search methods for general functions, convergence to the minimum cannot be guaranteed without an infinite number of evaluations. However, methods are available to estimate the value of the global minimum, allowing a designer to decide when an answer is satisfactory. It has long been known that, if random searches are carried out with a large number of test points, then

the probability function of the final result of the search (J_{final}) takes the form of a Weibull distribution.²⁰ The cumulative probability function for a Weibull distribution is

$$\Pr(J_{\text{final}} \leq x) = 1 - \exp\{-[(x-a)/b]^c\} \quad (28)$$

for $x \geq a \geq 0$, $b > 0$, and $c > 0$; a is the location parameter, b is the scale parameter, and c is the shape parameter; a is the minimum possible value of J_{final} ; in the context of function minimization, $a = J(d^*)$. If the search algorithm is run n times, n results of J_{final} are available to form an empirical probability function for J_{final} . Values of a , b , and c are found iteratively to give the least-squares difference between the Weibull distribution and the empirical distribution.

In Ref. 21, it is argued that the results of a randomized heuristic search algorithm have the same Weibull distribution as the results of a purely random search with many points. Golden²¹ uses the Weibull distribution to estimate $J(d^*)$ for the traveling-salesman problem. This work is expanded in Ref. 21 to give the confidence interval

$$\Pr[J_{\text{final},n} - b \leq J(d^*) \leq J_{\text{final},n}] = 1 - e^{-n} \quad (29)$$

where $J_{\text{final},n}$ is the best result of the n searches. Another procedure for estimating the value of $J(d^*)$ is developed by Cooke²² without assuming any specific form for the probability function. Cooke considers a sample of n random values, Y_i , and the associated cumulative probability function for the result of each sample, $\Pr(Y < x)$. The values are ordered such that Y_i is less than Y_{i+1} . The cumulative probability function for the maximum value Y_n is defined as $\Pr(Y_n < x)$ and is equal to $[\Pr(Y < x)]^n$. The expected value of the maximum of n samples is

$$E(Y_n) = \int_{x=Y_{\text{min}}}^{Y_{\text{max}}} x \text{pr}_{Y_n}(x) dx \quad (30)$$

where $\text{pr}_{Y_n}(x)$ is the probability density function corresponding to $[\Pr(Y_n < x)]$. By partial integration, Cooke obtains the estimator

$$\hat{Y}_{\text{max}} = 2Y_n - \sum_{i=0}^{n-1} \left\{ \left(1 - \frac{i}{n}\right)^n - \left[1 - \frac{(i+1)}{n}\right]^n \right\} Y_{n-i} \quad (31)$$

Using the relationship $Y = -J$, this gives an estimator for $J(d^*)$:

$$\hat{J}(d^*) = 2J_n - \sum_{i=0}^{n-1} \left\{ \left(1 - \frac{i}{n}\right)^n - \left[1 - \frac{(i+1)}{n}\right]^n \right\} J_{n-i} \quad (32)$$

where J_{i+1} is less than J_i . This method is computationally simple and gives an estimate for the parameter a .

Compensator Structure

The control signal is the sum of three components: the nominal trim value u_0 ; the increment needed to change the trim point to the new desired state, Δu^* ; and a dynamic component to ensure stability and shape the response, Δu_d .

The components Δu^* and Δu_d are developed by expressing Eqs. (4–8) in compact form and considering the first-order Taylor expansion about the trim point x_0 :

$$\dot{x} = f(x, u) \quad (33)$$

$$x = [V \quad \gamma \quad h \quad \alpha \quad q]^T \quad (34)$$

$$u = [\beta \quad \delta E]^T \quad (35)$$

$$x = x_0 + \Delta x \quad (36)$$

$$u = u_0 + \Delta u = u_0 + \Delta u^* + \Delta u_d \quad (37)$$

$$\dot{x} \approx f(x_0, u_0) + F \Delta x + G \Delta u = F \Delta x + G \Delta u \quad (38)$$

The Jacobian matrices $F = \partial f / \partial x$ and $G = \partial f / \partial u$ are evaluated at the trim condition.

Table 1 Stability and performance metrics

Metric	Definition
$I_{V,T25}$ ($I_{V,T50}$)	10% settling time greater than 25 s (50 s)
$I_{V,R25}$ ($I_{V,R50}$)	90% rise time greater than 25 s (50 s)
$I_{V,Rev}$	Reversal of response in V before peaking
$I_{V,D5}$ ($I_{V,D10}$)	10% dwell time more than 5 s (10 s)
$I_{V,OS10}$ ($I_{V,OS20}$)	Overshoot more than 10% (20%)
$I_{V,\Delta\alpha 0.5}$ ($I_{V,\Delta\alpha 1}$)	Maximum change in α more than 0.5 deg (1 deg)
$I_{V,g1}$ ($I_{V,g2}$)	Maximum load factor more than 1 g (2 g)
$I_{V,\Delta h 0.25}$ ($I_{V,\Delta h 0.5}$)	Maximum disturbance of h more than 0.25% (0.5%)
$I_{V,\delta T 50}$ ($I_{V,\delta T 100}$)	Maximum change in thrust more than 50% (100%)
$I_{V,\delta E 5}$ ($I_{V,\delta E 10}$)	Maximum change in elevator more than 5 deg (10 deg)

If Δy^* is the command vector and disturbances are neglected, then the equilibrium state Δx^* and control Δu^* are obtained from

$$\begin{bmatrix} \Delta x^* \\ \Delta u^* \end{bmatrix} = \begin{bmatrix} F & G \\ H_x & H_u \end{bmatrix}^{-1} \begin{bmatrix} 0 \\ \Delta y^* \end{bmatrix} \quad (39)$$

where $\Delta y^* = H_x \Delta x^* + H_u \Delta u^*$. For this example, the dynamic control laws are continuous-time, linear quadratic (LQ) regulators that provide proportional-integral (PI) compensation.² Integral compensation removes any steady-state error caused by the actual system differing from the model used in Eq. (39). However, transient response to command inputs can be improved by feedforward compensation, generating a need for both Δx^* and Δu^* . Furthermore, for nonlinear systems, it is important to keep control errors small, and providing reference values of the state and control is essential. This has been demonstrated widely by analyses, designs, and flight tests (also see Sec. 6.2 of Ref. 2).

For the hypersonic aircraft, the commanded states are velocity and height; therefore, the state vector is augmented as

$$\Delta x_{PI} = [\Delta V \quad \Delta \gamma \quad \Delta h \quad \Delta \alpha \quad \Delta q \quad \zeta_v \quad \zeta_h]^T \quad (40)$$

$$\zeta_v = \int (\Delta V - \Delta V^*) dt \quad (41)$$

$$\zeta_h = \int (\Delta h - \Delta h^*) dt \quad (42)$$

giving the LQ control law

$$\Delta u_d = -C_{PI} \Delta x_{PI} \quad (43)$$

where C_{PI} is the gain matrix. C_{PI} depends on the weights used in the integrand of the LQ cost function,

$$\mathcal{L} = \Delta x_{PI}^T Q \Delta x_{PI} + k_g V_0^2 \Delta x_{PI}^T F_y^T F_y \Delta x_{PI} + \Delta u_d^T R \Delta u_d \quad (44)$$

Q and R weight state and control deviations; for simplicity, they are defined as diagonal matrices. The term $k_g V_0^2 \Delta x_{PI}^T F_y^T F_y \Delta x_{PI}$ directly weights normal acceleration, which is closely approximated by $V_0 \dot{\gamma}$. Defining F_y as the row of F that corresponds to $\dot{\gamma}$, the normal acceleration is equal to $V_0 F_y \Delta x_{PI}$. The term k_g is a scalar cost-function weight.

Multiplying the control-gain matrix by a scalar constant k_C may improve robustness, though it distorts LQ optimality.²³ The final feedback law is, therefore,

$$\Delta u_d = -k_C C_{PI} \Delta x_{PI} \quad (45)$$

Ten design parameters were searched by the GA: k_g , k_C , diagonal elements of R , and six diagonal elements of Q (velocity weighting Q_V was fixed):

$$d = [Q_\gamma \quad Q_h \quad Q_\alpha \quad Q_q \quad Q_{\zeta_v} \quad Q_{\zeta_h} \quad k_g \quad R_\beta \quad R_{\delta E} \quad k_C] \quad (46)$$

The GA chooses Q and R weightings in the application, so the designer is absolved of this onerous task. As seen in the Stability and Performance Metrics section, it is easy to choose the 39 weights for engineering design metrics contained in the probabilistic cost function [Eq. (3)]. Extremely important metrics such as stability get high weights, e.g., 10; important metrics get intermediate weights, e.g., 1; and less important metrics get low weights, e.g., 0.1. In the example, Q and R are diagonal matrices, so the search is restricted to the diagonal elements. Off-diagonal elements of Q and R and state-control coupling could be accommodated either by expanding the search or by using the implicit-model-following structure mentioned at the end of this section. Positive definiteness of the matrices is ensured by the designer in specifying the search range of d , i.e., the search is not allowed to range over non-positive-definite values. Note, however, that if a bad choice of Q and R is made, the GA throws out that particular case on proceeding to the next generation. The most-fit compensator chosen by the GA has, by definition, satisfactory values of Q and R .

Initial values for d were chosen by selecting desired levels of deviation for Δx and Δu and setting the corresponding weights in Q and

R to be the squares of the inverses of the desired level.²⁴ For example, the expected variation in h is 2000 ft, and Q_h was set as $(\frac{1}{2000})^2$. The system response was propagated with these initial weights. The weights then were adjusted to produce a nominal response that violated only a few of the metrics. These parameter values provided the base point for the search, and a ± 1 -decade initial search range was set around each parameter.

The LQ-PI controller structure is used here to demonstrate the application of probabilistic robust control methods, and other control structures can be considered. Stochastic design based on proportional-integral-filter compensation has been applied to the hypersonic cruise problem,²⁵ and implicit-model-following flight controllers have been analyzed probabilistically.^{3,4} A probabilistic search for the coefficients of single-input/single-output compensator transfer functions is described in Ref. 26.

Results

Stochastic robustness analysis was used to illustrate open- and closed-loop robustness at the nominal flight condition ($M = 15$, $h = 110,000$ ft, $\gamma = 0$ deg, and $q = 0$ deg/s). Given the system parameter uncertainties described in Eqs. (14–25), there is a probability of 0.816 that the open-loop system will be unstable. The probabilities of violating the other metrics range between 0.816 and 1.

The base compensator yields a relatively low probability of closed-loop instability (0.014) and low probabilities of violating the performance metrics. Significant exceptions are the probabilities of settling-time violation: In response to a velocity command, $P_{V, T \leq 25} = 0.966$; in response to a height command, $P_{h, T \leq 50} = 1$.

Starting from the base compensator, the GA sought compensators optimized with respect to Eq. (27). Because stability robustness is important, the weighting is greatest on P_i (weight is equal to 10). Weights of 1 were chosen for the metrics that indicate particularly poor performance, e.g., settling time greater than 50 s; weights of 0.1 were chosen for metrics that indicate moderate performance, e.g., settling time greater than 25 s.

The optimization begins with an initial random search. After the random search, the GA refines the population over several generations until a stopping condition is met. For this example, the search was stopped when more than 20,000 MCEs had been used. The algorithm was run eight times to estimate the global minimum, e.g., Eq. (32). The final values of \hat{J} for each of the eight runs were 2.09, 1.86, 2.16, 2.71, 1.99, 1.83, 1.72, and 1.74; hence, the seventh run gave the best result.

The global minimum estimate can be made in two ways: by fitting a Weibull distribution to the results [Eq. (28)] or by using Cooke's estimate [Eq. (32)]. Here, both methods are used together. On the basis of the eight final values of \hat{J} , Eq. (32) estimates the value of the global minimum to be 1.703. To corroborate this result, it is used as the parameter a in the Weibull distribution [Eq. (28)]. The eight observed results are used to estimate the cumulative probability function of the results of the GA, and values for b and c are chosen to fit Eq. (27) to the observed results, giving $a = 1.703$, $b = 0.28$, and $c = 0.8$. The results of the eight runs and the fitted Weibull function are shown in Fig. 2. We conclude that the estimate of 1.703

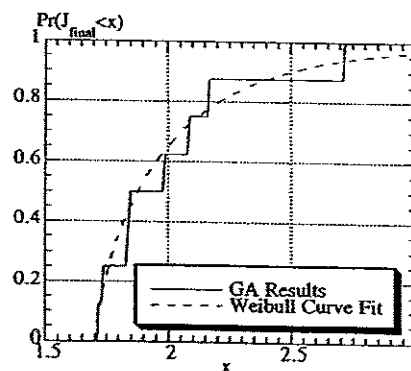


Fig. 2 Comparison of empirical results with assumed Weibull distribution.

for the global minimum is a viable value for a . If we assume that the estimate for b is accurate, then Eq. (29) gives

$$\Pr[1.72 - 0.28 \leq J(d^*) \leq 1.72] = 1 - e^{-8} = 0.9997 \quad (47)$$

We therefore have an estimate that the global minimum is 1.703, and we are 99.97% certain that the global minimum has a value between 1.44 and 1.72. Furthermore, if we accept the estimate that, given this compensator structure, the best achievable value of J is 1.703, then the compensator produced by the seventh run, with a value of 1.72, has a cost within 1% of the global minimum.

The method of analysis and design is computationally intensive, although the computational burden is well within the capabilities of existing computers. Using MATLAB® running on a Silicon Graphics Indy workstation, the computation time required to design a compensator for this paper was about 24 h. Translated to C or Fortran for a state-of-the-art parallel computer, run times would be measured in minutes or seconds.

The generic robust control problem is computationally complex: Run times for exact solutions are exponential in the number of variables, and the number of variables is infinite for even a single, continuously distributed uncertain parameter. Consequently, all robust design methods must be approximate to some degree. The stochastic approach presented here uses Monte Carlo simulation for evaluation and numerical search for design. MCE of eigenvalues and response histories is accomplished with run times that are polynomial in the number of state and control elements and linear in the simulated response time and number of uncertain parameters. GA run times are linear in the number of design constants to be found by search.

There are a number of ways to extend the flight control system design across the entire flight envelope. For the LQ design approach used here, the most likely way is to use gain scheduling. For example, the second author and his colleagues developed and flight-tested gain-scheduled, digital, linear-quadratic-Gaussian controllers for a tandem-rotor helicopter in the mid-1970s, demonstrating excellent real-time performance across the tested flight envelope (including hover and rearward flight as well as climbs, turns, and level cruising flight).^{27,28}

Analysis of the Optimized Compensator

The robustness profiles for the base compensator and the optimized compensator are compared graphically in Fig. 3. The probability of instability drops from 0.014 to 0.001. The probabilities of settling-time violation improve by factors of 4.5 ($P_{V,T50}$) and 1.02 ($P_{h,T500}$), although $P_{h,T500}$ remains equal to one. All of the other metrics improve except three: the probability of using more than 50% throttle after the velocity command step ($P_{V,5750}$) and the probability of load factors greater than 2 or 4 after the height command step ($P_{h,g2}$, $P_{h,g4}$).

The 0.1% probability of instability would be, of course, worrying for an aircraft system. The probability could be reduced by increasing the weight on P_i in Eq. (27), allowing cross-product weighting in the LQ cost function, or considering alternate control structures. However, the P_i will never be zero if the parameters have normal distributions. This is a property of the underlying problem and the associated $\text{pr}(\nu)$, not a property of the compensator. To illustrate this, the compensator was reanalyzed with bounded parameter distributions: normal distributions bounded at ± 0.2 . (The standard

deviation in the earlier analysis was 0.1.) In this case, the estimated probability of instability is precisely zero. This also reinforces the importance of understanding the likely forms of parameter variation in each application.

With the nominal parameters, the closed-loop eigenvalues of the base compensator are located at $-1.1956 \pm 0.9184i$, $-0.0210 \pm 0.0213i$, -0.0415 , -0.0064 , and -0.0004 . For the optimized system, the eigenvalues are at $-1.0025 \pm 1.3383i$, $-0.0219 \pm 0.0186i$, -0.0408 , -0.0088 , and -0.0044 . The most significant difference is an 11-fold increase in the speed of the integral mode: its eigenvalue moves from -0.0004 to -0.0044 .

The effects of plant parameter uncertainties on the closed-loop system are shown graphically using stochastic root loci, as in Figs. 4 and 5. This graphical tool gives designers qualitative information on how parameter variations may change the system response. The optimized compensator roots (Fig. 5) have less scatter than the baseline compensator roots (Fig. 4) and are more solidly located in the left-half plane. Further insights can be gained by using graphs of the conditional probabilities of metric violation.^{8,25} Graphs can be recorded for each robustness metric and for each parameter. Figure 6

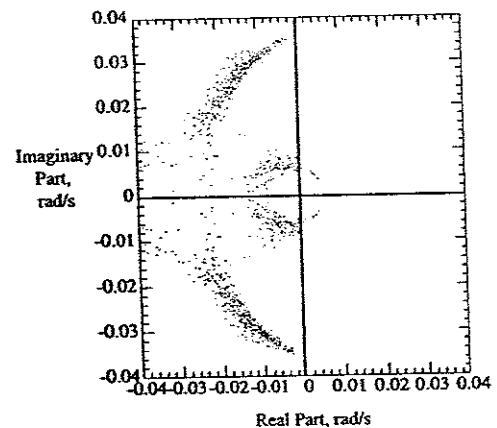


Fig. 4 Stochastic root locus of baseline compensator.

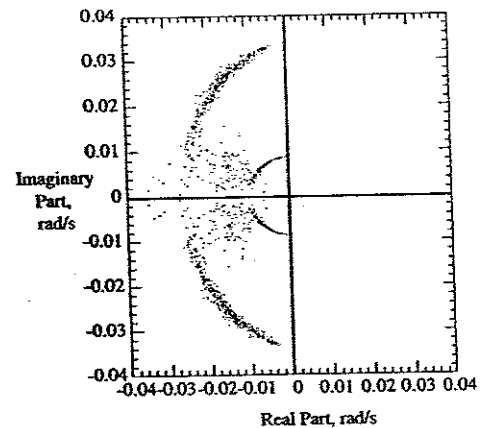


Fig. 5 Stochastic root locus of optimized compensator.

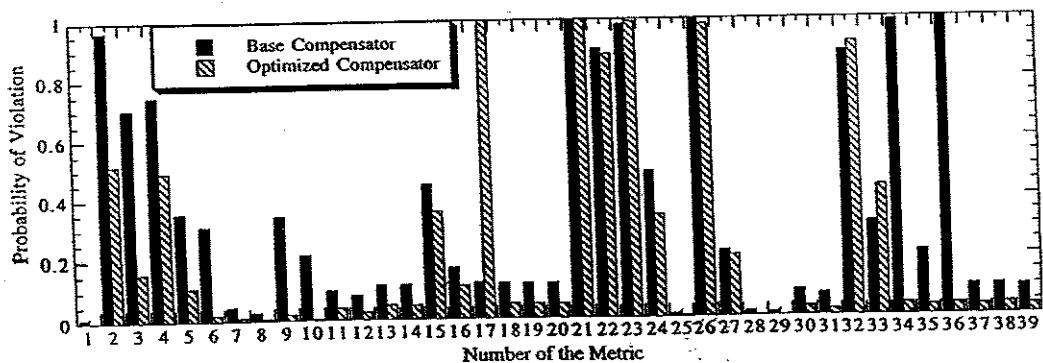


Fig. 3 Comparison of the robustness profiles of the base and optimized compensators.

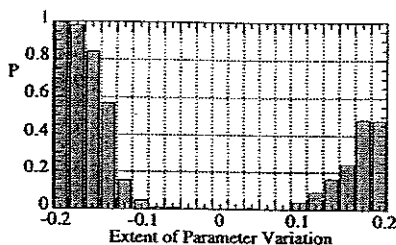


Fig. 6 Conditional probability of violating the settling-time metric as air density estimate (parameter ν_8) changes.

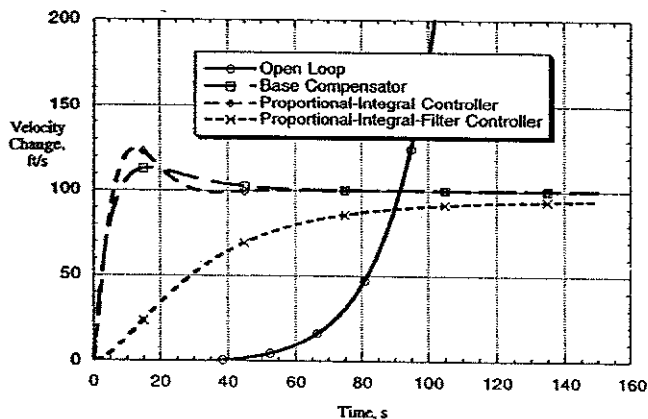


Fig. 7 Velocity response to a 100-ft/s step-velocity command.

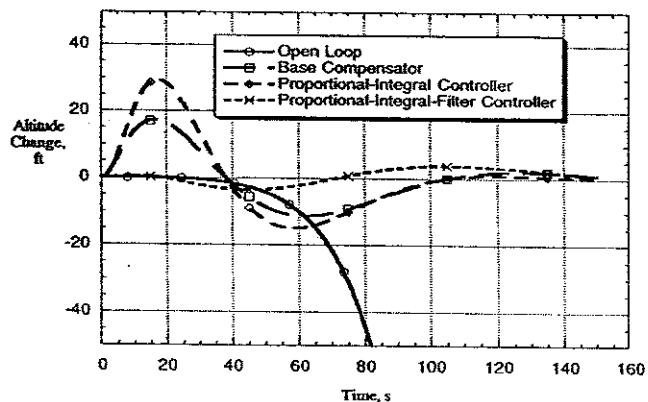


Fig. 8 Altitude response to a 100-ft/s step-velocity command.

shows the effect of parameter ν_8 , the uncertainty in the air density estimate, on the probability of the settling time being greater than 50 s in response to a velocity command ($I_{V, T=50}$). If ν_8 varies from the nominal value by less than ± 0.1 , then the metric will almost never be violated; however, the metric will always be violated if ν_8 varies by -0.2 , illustrating the importance of good knowledge of air density.

The robustness profiles can be adjusted by changing the control structure or by changing the weights in the robustness cost function [Eq. (27)]. In Ref. 25, proportional-integral-filter compensation also is implemented; it removes the peaks in throttle and elevator usage but results in a slightly higher probability of instability. Velocity and altitude responses to a 100-ft/s step-velocity command are compared in Figs. 7 and 8. Changing the weights in Eq. (27) allows the designer to make direct tradeoffs between elements of the robustness profile and to tailor the design to the application.²⁵

Conclusions

Stochastic robustness is shown to provide an effective basis for flight control system design and analysis. The method is demonstrated on a problem that possesses significant nonlinearity, 28 uncertain parameters, and 39 stability and performance specifications. Ten control design parameters are found using a genetic algorithm, and an estimate of optimality is obtained by fitting multiple results to a Weibull distribution. Most synthesis methods would find such a task daunting; however, stochastic robustness synthesis provides

a straightforward framework and allows a range of robust compensators to be designed. The genetic algorithm produced compensators that approach the best performance achievable for the given control structure.

References

- Kalos, M. H., and Whitlock, P. A., *Monte Carlo Methods*, Wiley, New York, 1986.
- Stengel, R. F., *Optimal Control and Estimation*, Dover, New York, 1994 (originally published as *Stochastic Optimal Control: Theory and Application*, Wiley, New York, 1986).
- Ray, L., and Stengel, R. F., "Application of Stochastic Robustness to Aircraft Control Systems," *Journal of Guidance, Control, and Dynamics*, Vol. 14, No. 6, 1991, pp. 1251-1259.
- Ray, L. R., and Stengel, R. F., "Stochastic Measures of Performance Robustness in Aircraft Control Systems," *Journal of Guidance, Control, and Dynamics*, Vol. 15, No. 6, 1992, pp. 1381-1387.
- Ray, L. R., and Stengel, R. F., "Stochastic Robustness of Linear-Time-Invariant Control Systems," *IEEE Transactions on Automatic Control*, Vol. 36, No. 1, 1991, pp. 82-87.
- Ray, L. R., "Stochastic Robustness of Linear Multivariable Control Systems: Towards Comprehensive Robustness Analysis," Ph.D. Thesis, Dept. of Mechanical and Aerospace Engineering, Princeton Univ., Princeton, NJ, Jan. 1991.
- Ray, L. R., and Stengel, R. F., "A Monte Carlo Approach to the Analysis of Control System Robustness," *Automatica*, Vol. 29, No. 1, 1993, pp. 229-236.
- Stengel, R. F., and Marrison, C. I., "Robustness of Solutions to a Benchmark Control Problem," *Journal of Guidance, Control, and Dynamics*, Vol. 15, No. 5, 1992, pp. 1060-1067.
- Marrison, C. I., and Stengel, R. F., "Reply by Authors to J. J. Gribble," *Journal of Guidance, Control, and Dynamics*, Vol. 18, No. 6, 1995, pp. 1468-1470.
- Marrison, C. I., and Stengel, R. F., "Stochastic Robustness Synthesis Applied to a Benchmark Control Problem," *International Journal of Robust and Nonlinear Control*, Vol. 5, No. 1, 1995, pp. 13-31.
- Marrison, C. I., and Stengel, R. F., "Robust Control System Design Using Random Search and Genetic Algorithms," *IEEE Transactions on Automatic Control*, Vol. 42, No. 6, 1997, pp. 835-839.
- Fitzpatrick, J. M., and Grefenstette, J. J., "Genetic Algorithms in Noisy Environments," *Machine Learning*, Vol. 3, No. 2-3, 1988, pp. 101-120.
- Goldberg, D. E., *Genetic Algorithms in Search, Optimization, and Machine Learning*, Addison-Wesley, Reading, MA, 1989.
- Holland, J., *Adaptation in Natural and Artificial Systems*, Univ. of Michigan Press, Ann Arbor, MI, 1975.
- Krishnakumar, K., "Genetic Algorithms: An Introduction and an Overview of Their Capabilities," *Proceedings of the AIAA Guidance, Navigation, and Control Conference*, AIAA, Washington, DC, 1992, pp. 728-738 (AIAA 92-4462).
- Rogers, G. F. C., and Mayhew, Y. R., *Thermodynamic and Transport Properties of Fluids*, Blackwell, Oxford, England, UK, 1981.
- Shaughnessy, J. D., Pinckney, S. Z., Memmin, J. D., Cruz, C. I., and Kelley, M.-L., "Hypersonic Vehicle Simulation Model: Winged-Cone Configuration," NASA TM 102610, Nov. 1990.
- Stengel, R. F., "Altitude Stability in Supersonic Cruising Flight," *Journal of Aircraft*, Vol. 7, No. 5, 1970, pp. 464-473.
- Hahn, W., *Theory and Application of Liapunov's Direct Method*, Prentice-Hall, Englewood Cliffs, NJ, 1963.
- Fisher, R., and Tippett, L., "Limiting Forms of the Frequency Distribution of the Largest or Smallest Member of a Sample," *Proceedings of the Cambridge Philosophical Society*, Vol. 24, 1928, pp. 180-190.
- Golden, B. L., "Interval Estimation of a Global Optimum for Large Combinatorial Problems," *Naval Research Logistics Quarterly*, Vol. 26, No. 1, 1979, pp. 69-77.
- Cooke, P., "Statistical Inference for Bounds of Random Variables," *Biometrika*, Vol. 66, No. 2, 1979, pp. 367-374.
- Wong, P. K., and Athans, M., "Closed-Loop Structural Stability for Linear-Quadratic Optimal Systems," *IEEE Transactions on Automatic Control*, Vol. AC-22, No. 1, 1977, pp. 94-99.
- Bryson, A. E., and Ho, Y. C., *Applied Optimal Control*, Hemisphere, Washington, DC, 1975.
- Marrison, C. I., "The Design of Control Laws for Uncertain Dynamic Systems Using Stochastic Robustness Metrics," Ph.D. Thesis, Dept. of Mechanical and Aerospace Engineering, Princeton Univ., Princeton, NJ, Jan. 1995.
- Stengel, R. F., and Wang, Q., "Searching for Minimal-Order Robust Compensators" (manuscript in preparation).
- Stengel, R. F., Broussard, J., and Berry, P., "Digital Controllers for VTOL Aircraft," *IEEE Transactions on Aerospace and Electronic Systems*, Vol. AES-14, No. 1, 1978, pp. 54-63.
- Stengel, R. F., Broussard, J., and Berry, P., "Digital Flight Control Design for a Tandem-Rotor Helicopter," *Automatica*, Vol. 14, No. 4, 1978, pp. 301-311.